

1 Performance Characterization of Asphalt Mixture Modified with One- 2 component Polyurethane

3 Guoyang Lu^a, Rui Li^b, Gaoyang Li^b, Zhen Leng^b, Haopeng Wang^{c*}

4 ^a *Department of Architecture and Civil Engineering, The City University of Hong Kong,*
5 *Hong Kong, China*

6 ^a *Department of Civil and Environmental Engineering, The Hong Kong Polytechnic*
7 *University, Hong Kong, China*

8 ^b *Nottingham Transportation Engineering Centre (NTEC), Faculty of Engineering,*
9 *University of Nottingham, Nottingham, United Kingdom*

10 *Corresponding author. Email: haopeng.wang@nottingham.ac.uk

11 **Abstract:** Using polyurethane (PU) modified asphalt for paving purposes has
12 recently gained increasing interest in both academia and industry. This study aims
13 to characterize the engineering performance of the asphalt mixture modified with
14 one-component PU and explore its adhesive mechanism. To achieve this objective,
15 PU modified bitumen and asphalt mixture of two different PU contents (10% and
16 30%) were prepared. Various laboratory material property tests, such as rotational
17 viscosity test of binder, Marshall test, indirect tensile strength test, Hamburg
18 wheel-tracking test, moisture susceptibility, and indirect tensile fatigue test of PU
19 modified mixture, were performed. Fourier transform infrared spectroscopy test
20 was carried out to explore the adhesive mechanism between PU-modified binder
21 and aggregate. The results indicated that the overall performances of asphalt
22 mixture were increased significantly by PU prepolymer, including increased
23 Marshall stability, indirect tensile strength, and resistance to moisture damage,
24 rutting and fatigue damage. It was found that PU prepolymer can react with the
25 hydroxyl groups on the aggregate surface, which contributed to better performance
26 of asphalt mixture. The findings of this study may facilitate the further practical
27 applications of one-component PU-modified bituminous materials in the pavement
28 industry.

29 **Keywords:** polyurethane; performance characterization; adhesive; bitumen &
30 tar; pavements & roads; UN SDG 9

31 **1 Introduction**

32 Growing needs in mobility and the simultaneous decrease of natural resources require
33 innovative and sustainable solutions in terms of transportation infrastructure. As a major
34 type of transportation infrastructure, pavements are expected not only to carry more
35 traffic load (longer durability), but also to provide sustainable benefits (such as low
36 energy consumption and emission).

37 To meet the increasing requirements of pavement materials for future mobility,
38 the incorporation of polymers, such as styrene-butadiene-styrene (SBS), crumb rubber
39 (CR), polyethylene terephthalate (PET), and epoxy, in asphalt materials has been
40 extensively studied. By adding these polymers, the properties of asphalt will be improved
41 to varying degrees, and the durability of the pavement will be enhanced (Wang et al.,
42 2020b, Leng et al., 2018, Airey, 2003, Wang et al., 2020a). However, there are still some
43 environmental issues that need to be addressed. For instance, the blending and swelling
44 of polymers in asphalt need high production temperatures, which consumes more energy,
45 and the potential greenhouse gas emissions and the associated air pollutions from the
46 asphalt binder and polymer itself at high construction temperatures have not been well
47 studied (Zhu et al., 2019, Wang et al., 2018, Cao et al., 2019).

48 In recent years, polyurethane (PU) has been studied as a binder modifier to
49 provide pavement materials with both superior functional properties and good mechanical
50 performance (Hong et al., 2021a, Lu et al., 2019). PU binder is a compound containing
51 urethane groups (-NHCOO-) in molecule chains stemming from the reaction of
52 isocyanate-based materials (containing -NCO functional groups) with polyols (containing
53 -OH groups). Due to the low viscosity of PU binder, it can be applied readily at ambient
54 temperature. Hence, during the manufacturing process of PU pavement mixture, no
55 heating is required, and the green-house gas (GHG) emissions can be eliminated (Cong

56 et al., 2019, Chen et al., 2018). As a sustainable and durable pavement material, PU binder
57 has been extensively researched and its performance has been widely validated in
58 engineering practices (Jin et al., 2020, Hong et al., 2021b).

59 However, due to the unit price of PU is much higher than that of asphalt, to
60 completely replace asphalt by PU binder becomes impossible, except for some special
61 application scenarios, which hinders the wider application of PU in practice. To address
62 this problem, the application of PU-precursor-based or PU-based materials as a reactive
63 asphalt modifier was further investigated (Fang et al., 2016, Singh et al., 2003). PU-
64 precursor-based modifier (PUM) containing isocyanate functionalities (contain -NCO
65 functional groups) can easily react with various compounds containing functional groups
66 such as hydroxyl groups or amino groups. Due to the wide presence of free radicals (such
67 as -OH, -NH, -NH₂) in asphalt, the use of PUM was proved as a chemical modification
68 for asphalt. PUM also presents good compatibility with asphalt (Li et al., 2021), which
69 can significantly improve the high-temperature performance and fatigue resistance of
70 asphalt. Since PUM commonly used for asphalt modification is a liquid modifier, there
71 is no need to use a colloid mill to grind the modifier when preparing the modified asphalt
72 binder. Compared with other solid modifiers, the production process is simpler. At the
73 same time, due to the good fluidity of PUM, the mixing temperature for producing
74 modified asphalt can also be reduced from the conventional 180°C to about 140°C (Li *et*
75 *al.* 2021). Therefore, the use of PUM to prepare modified asphalt not only reduces the
76 production cost, but also decreases the GHG emissions in the production process.

77 Although the properties and performance of asphalt binder modified by PUM
78 have been reported in some previous studies, the preparation processes and performance
79 of such PUM modified asphalt mixtures (PUAM) have not been comprehensively
80 characterized yet. Therefore, to further verify the applicability of PUM in pavement

81 materials, the engineering performances of PUAM should be thoroughly studied. In
82 addition, a suitable production process for PUAM needs to be determined, and a better
83 understanding on the chemo-mechanical interactions between PUM, asphalt and
84 aggregates should be obtained.

85 To fill these gaps, this study aims to characterize the engineering performance and
86 reveal the modification mechanism of PUAM. To achieve this objective, a PUM was
87 selected to produce PU modified binder (PUMB) and PUAM of two different PU contents
88 (10% and 30%). Various laboratory tests, including rotational viscosity tests of binder,
89 and Marshall test, indirect tensile strength (ITS) test, Hamburg wheel-tracking test,
90 moisture susceptibility, and indirect tensile fatigue (ITF) test of mixture, were performed.
91 Fourier transform infrared spectroscopy test was carried out to investigate the adhesive
92 mechanism between binder and aggregate. The outcome of this study is expected to lay
93 the foundation for the further application of PUAM in larger scales.

94 **2 Materials and methodology**

95 **2.1 Materials**

96 *2.1.1 Polyurethane prepolymer*

97 The PU prepolymer selected in this study is a solvent-free, unfilled and transparent 1k
98 aliphatic polyurethane. It is a moisture curing adhesive. The basic physical properties of
99 the PU prepolymer are shown in **Table 1**.

100 *2.1.2 Base binder and aggregate*

101 The penetration 60/70 binder (Pen 60/70), commonly used in Hong Kong, was selected
102 as the base binder. Its basic properties are shown in **Table 2**. The aggregate and filler
103 used in this research are both granites. The bulk densities of coarse aggregate, fine
104 aggregate and mineral filler are 2.663, 2.649, 2.661 g/cm³.

105 **2.2 Preparation of polyurethane (PU) modified bitumen**

106 The base bitumen was first heated to approximately 160 °C in an oven to achieve good
107 fluidity. The PU prepolymer in target amount was then mixed with the fluid bitumen. To
108 ensure homogeneity of the PU modified bitumen, high shear mixer was used to mix the
109 blend at 150 °C at a speed of 3000 rpm for 30 min. PU was added to the bitumen at two
110 different dosages, i.e., PU prepolymer: bitumen = 10:90, and 30:70, which are denoted as
111 PUMB-10 and PUMB-30, respectively. The base binder Pen 60/70 was used as control.

112 In order to study the reaction mechanism of the PU modified asphalt mixture, the
113 PU modified bitumen mastic was prepared by mixing the PU modified bitumen with dried
114 mineral filler at a mass ratio of 1:1.5, which is close to their mass ratio in the asphalt
115 mixture. The mastic was sealed in a closed centrifuge tube, which was then conditioned
116 in an oven at 60 °C for up to 48 h (Si et al., 2018). The infrared spectra of the mastic
117 during the conditioning were measured after 0 h, 12 h, 24 h, and 48 h conditioning.

118 **2.3 Mix design of PU asphalt mixture**

119 The typical gradation for the 20mm maximum aggregate size wearing course mixture
120 (WC 20) used in Hong Kong was selected in this study to prepare the asphalt mixtures,
121 as illustrated in **Figure 1**.

122 **2.4 Mixture specimen preparation**

123 Two types of PU asphalt mixture (PUAM) with different PU contents were prepared in
124 this study: PUAM-10 and PUAM-30, which correspond to the mass ratios of PU
125 prepolymer to virgin binder of 10:90 and 30:70, respectively. The hot mix asphalt (HMA)
126 mixture prepared with Pen 60/70 binder was also produced as a reference mixture to
127 investigate the improvement of the mechanical properties of PUAM.

128 For PUAM, the warm mix method was adopted to prepare the mixtures, and the
129 mixing and compacting temperatures were reduced to 160°C and 140°C respectively.

130 The mixture specimens were prepared in accordance with ASTM D6926-10.
131 From the Marshall test results and various volumetric parameters, the optimum asphalt
132 contents for HMA, PUAM-10, and PUAM-30 were determined to be 5.2%, 5.3%, and
133 5.3%, respectively.

134 Since PU is a reactive modifier, similar to the epoxy resin (Apostolidis et al., 2018,
135 Yang et al., 2022), it needs curing to develop its strength after the sample preparation.
136 Therefore, after demolding, the PUAM specimens were cured in a 60°C oven for 4 days
137 according to the curing method of epoxy asphalt mixtures (Yin *et al.* 2015, Cong *et al.*
138 2019).

139 **2.5 Laboratory tests**

140 *2.5.1 Rotational viscosity*

141 The rotational viscosity of the binders was measured in accordance with ASTM D4402
142 at 150 °C at a constant rotational speed of 20 rpm using the #27 cylindrical spindle
143 (spindle diameter=11.76 mm, side length=33.02 mm, effective length=39.29 mm) (Wang
144 et al., 2021). It was reported that potential chemical reaction between the PU prepolymer
145 and base bitumen will lead to dramatic viscosity change of the binder (Li et al., 2022). To
146 further evaluate whether there is any chemical reaction occurs, the viscosity of PU
147 modified binders was continuously monitored at 150 °C for up to 120 min.

148 *2.5.2 Fourier transform infrared (FTIR) spectroscopy*

149 Attenuated total reflection ATR-FTIR (Spectrum Two, PerkinElmer) was used to analyse
150 the FTIR spectra of the PU modified bitumen and mastics with a 4 cm⁻¹ resolution
151 between 400 and 4,000 cm⁻¹. Each spectrum represents the accumulation of 32 scans.
152 Two measurements were performed for each specimen.

153 *2.5.3 Marshall test*

154 Marshall test was conducted to measure the Marshall stability and flow values of asphalt
155 mixture according to ASTM-D6927. The optimum asphalt content was also determined
156 by this test. Specimens were first immersed in a 60°C water bath for 30-40 min. Then a
157 loading with a constant displacement rate of 50.8 mm/min was applied to the specimens.
158 Three replicates were prepared for each group and the maximum load and flow values
159 were recorded.

160 *2.5.4 Indirect tensile strength test*

161 The indirect tensile strength (ITS) of the asphalt mixture was measured according to
162 AASHTO T322. The testing temperature was 25°C, and a vertical compressive load with
163 a 50±5 mm/min displacement rate was applied to the testing samples until the maximum
164 load was reached. The ITS values of the specimens in MPa were calculated by Eq. (1):

165
$$ITS = \frac{2000P}{1000 \cdot \pi \cdot D \cdot t} \quad (1)$$

166 where P is the maximum load applied to the specimens (N), and t and D are the thickness
167 and diameter of the specimens (mm), respectively.

168 *2.5.5 Hamburg wheel-tracking test*

169 Hamburg wheel-tracking test was conducted to evaluate the rutting resistance of asphalt
170 mixture according to AASHTO T 324-11. The cylindrical specimens with 150 mm
171 diameter, 60±1 mm height, and 7±1 % air voids content were prepared by a Superpave
172 Gyratory Compactor (SGC). The test was conducted in a 60°C water bath and a repeated
173 load of 705±4.5 N generated by the reciprocating steel wheel was applied to the
174 specimens. The rut depth and the number of passes to specimen failure were recorded.
175 The test stopped when the number of passes reached 20000 or the specified rutting depth
176 was reached.

177 *2.5.6 Moisture susceptibility*

178 The freeze-thaw splitting test was adopted to estimate the moisture susceptibility of the
179 asphalt mixture. Six cylindrical specimens with $7\pm 1\%$ air voids content were prepared for
180 testing. Following the procedure recommended by ASTM D4867, three conditioned
181 specimens were partially saturated with water and placed in a -18°C freezer for 16 h, and
182 then immersed in a 60°C water bath for another 24 h. This process aims to simulate the
183 damage caused by the water in the asphalt mixture after a freeze-thaw cycle. After freeze-
184 thaw conditioning, the ITS test was performed on two subsets of specimens at 25°C to
185 obtain the indirect tensile strength values. Tensile stress ratio (TSR), defined as the ratio
186 of ITS of conditioned specimens to unconditioned specimens, as shown in Eq. (2), was
187 used to evaluate the moisture susceptibility of asphalt mixtures.

188
$$\text{TSR} = \frac{ITS_{con}}{ITS_{uncon}} \cdot 100 \quad (2)$$

189 where ITS_{con} is the average tensile strength of the moisture conditioned subset, and
190 ITS_{uncon} is the average tensile strength of the unconditioned subset.

191 *2.5.7 Indirect tensile fatigue (ITF) test*

192 The fatigue life of the asphalt mixture was determined by the indirect tensile fatigue (ITF)
193 test. The testing temperature was 20°C and the tests were conducted in a stress-controlled
194 mode. A haversine load was applied on the specimen repeatedly with 0.1s loading time
195 and 0.4s rest time. As recommended by BS EN 12697-24, five initial resilient strain levels
196 were selected from the range of $70\mu\epsilon$ to $400\mu\epsilon$ for fatigue testing. However, because the
197 strength of PUAM-30 is very high, it requires more than 2000kPa stress to make the initial
198 strain within the recommended range, which is quite different from the actual load applied
199 on road in a real situation. The pressure between the tire of a standard vehicle and the
200 pavement is 700kPa . Based on this value, this study selected three stress levels of 800kPa ,
201 600kPa , and 400kPa for the ITF test. Three replicates were prepared for each stress level

202 to ensure the consistency of the results. The fatigue life is the number of load applications
203 corresponding to the maximum energy ratio, and the energy ratio is calculated by Eq. (3):

$$204 \quad w_n = \frac{n}{\varepsilon_{R,n}} \cdot 10^6 \quad (3)$$

205 where w_n is the energy ratio; n is the number of load applications, and $\varepsilon_{R,n}$ is the resilient
206 strain amplitude during cyclic loading ($\mu\text{m/m}$).

207 **3 Results and discussions**

208 **3.1 Rotational viscosity**

209 The rotational viscosity of the base bitumen and PU modified bitumen was tested after
210 sample preparation. The viscosity was recorded after shearing for around 20 min, until
211 the value became stable. It can be seen from **Table 3** that the viscosity decreased with the
212 incorporation of PU prepolymer, as the PU prepolymer has lower viscosity compared
213 with that of the base bitumen.

214 **Figure 2** shows the shear viscosities of both PUMB-10 and PUMB-30 as a function of
215 time at 150 °C for up to 120 min. The viscosity of the PUMB was relatively stable during
216 the monitoring duration. It was reported that potential chemical reaction between the PU
217 prepolymer and base bitumen will lead to dramatic viscosity change of the binder (Li et
218 al., 2022). The result indicates that the chemical reaction between PU prepolymer and
219 bitumen is insignificant.

220 **3.2 Marshall and volumetric properties**

221 The Marshall stability test results are presented in **Figure 3**. It can be observed that the
222 stability of PUAM is higher than that of the HMA mixture and it increases with the
223 increase of PU content. PUAM-10 has a stability of 22.8 kN, a 50% increase over 15.7kN
224 of the HMA mixture. For PUAM-30, its stability is higher than 50kN (limited by the
225 machine measuring range), which is more than three times that of the HMA mixture. The

226 improvement of PUAM stability suggests that the high-temperature deformation
227 resistance of the asphalt mixture has been greatly strengthened after PU modification.
228 The volumetric parameters of the mixtures are shown in **Table 4**. The air void content of
229 PUAM is larger than that of the HMA mixture. With the increase of PU content, the air
230 void of PUAM also increased. The possible reason is that PU is an active reactive
231 modifier, which is easy to react with those substances containing active hydrogen groups,
232 such as mineral aggregates, asphalt binder and moisture in the air, during the preparation
233 process. This reaction (curing) makes the loose mixture stick together, gradually reduces
234 the workability of the mixture, resulting in decreased compaction degree. However, it can
235 be seen that, although the air void content of PUAM-30 is larger than those of the other
236 two mixtures, its mechanical strength is still the highest, revealing the PU prepolymer can
237 significantly enhance the strength of asphalt mixture.

238 ***3.3 Indirect tensile strength***

239 **Figure 4** compares the indirect tensile strength of the HMA mixture and PUAM. The ITS
240 of PUAM is higher than that of the HMA, and its value increases with the increase of PU
241 content. It can be noticed from **Figure 4** that the ITS of PUAM-30 is almost twice of that
242 of the control HMA. This denotes that the PU prepolymer contributes to the higher tensile
243 strength. It is believed that the PU prepolymer enhances the adhesion between the asphalt
244 binder and the aggregates, thus improving the tensile properties of the asphalt mixture.
245 Based on this result, the PUAM is expected to have better cracking resistance than the
246 HMA.

247 ***3.4 Rutting resistance***

248 **Figure 5** shows the rutting depth evolutions of different asphalt mixture samples with the
249 increasing number of loading passes. It can be found that the rutting depth of the control
250 asphalt mixture sample increases dramatically with the increase of loading passes. On the

251 other hand, with the incorporation of PU prepolymer, the rutting depth decreased
252 remarkably. The rutting depth of the control asphalt mixture reached 20 mm at the end of
253 the test, while it was less than 2 mm and 1 mm for PUAM-10 and PUAM-30, respectively.
254 **Figure 6** shows the pictures of the test samples after the wheel-tracking tests, which
255 clearly illustrate the improvement of rutting resistance of PUMA.

256 ***3.5 Moisture susceptibility***

257 The results of the moisture susceptibility tests are plotted in **Figure 7**. It can be seen that
258 PUAM-30 has the highest TSR value, indicating PUAM-30 has the best moisture
259 susceptibility resistance among these three mixtures. The strength of the unconditioned
260 HMA mixture, PUAM-10, and PUAM-30 are 13.1kN, 16.2kN, and 21.1kN, respectively.
261 After freeze-thaw cycling, the strength of HMA dropped to 7kN, and its tensile stress
262 ratio is only 53%, which is far from the required value of 80%. Concerning PUAM, there
263 is only a slight decrease in strength after conditioning, especially for PUAM-30. The
264 strength of conditioned PUAM-10 and PUAM-30 are 14.4kN and 20kN, and their
265 corresponding TSR values are 90% and 95%. This result indicates that PU prepolymer
266 can effectively improve the resistance of moisture damage of asphalt mixture.

267 ***3.6 Fatigue performance***

268 **Figure 8** illustrates the fatigue test results of the PUAM and HMA under three stress
269 levels, which show that the fatigue performance of PUAM was significantly better than
270 that of the HMA, and the degree of the improvement is proportional to the PU dosage. At
271 800kPa stress level, the fatigue life of the PUAM-10 is 12284 cycles, while the HMA is
272 only 422 cycles. As the applied stress decreases, the advantage of the fatigue performance
273 of PUAM-10 becomes more obvious. This result demonstrates that the PUAM-10
274 exhibits much better fatigue performance than the HMA. For PUAM-30, due to its high
275 mechanical property, even under 800kPa stress, the modulus did not change after 100000

276 loading cycles, meaning that the fatigue load caused nearly no damage to it. For this
277 reason, the ITF tests of PUAM-30 under the three loading stress levels were manually
278 stopped after 100000 loading cycles.

279 To more specifically display the relationship between modulus and loading cycles
280 for PUAM and HMA, **Figure 9** depicts the profiles of modulus change with loading
281 cycles. Regardless of the stress levels, the modulus of PUAM-30 almost did not decrease
282 with the increase of loading cycles, indicating that the specimen hardly suffered fatigue
283 damage during the loading process. For PUAM-10, it can be seen that under a stress level
284 of 400kPa, its modulus was also very stable with the increase of loading cycles. However,
285 under the stress level of 600kPa and 800kPa, its modulus decreased apparently with the
286 increase of loading cycles, indicating damage accumulated in the samples. However, the
287 decreasing rate is significantly smaller than the control HMA mixture. From the above
288 results, it can be concluded that the fatigue performance of the HMA can be significantly
289 enhanced by PU prepolymer, especially for PUAM-30.

290 **3.7 PU modification mechanism**

291 **Figure 10** presents the FT-IR spectra of the base bitumen Pen 60/70 and PU modified
292 bitumen binders (PUMB-10 and PUMB-30). The commonly seen bands in PU modified
293 bitumen binders are summarized in **Table 5**. The distinct peak at 2270 cm^{-1} corresponding
294 to the stretching of the isocyanate group (-NCO) increased significantly with larger
295 concentration of PU prepolymer. The peaks at 1725 cm^{-1} and 1529 cm^{-1} are attributed to
296 the absorption of the carbonyl group (C=O stretching) and the imino group (N-H bending),
297 respectively, indicating the presence of amide group in PU prepolymer. In addition, the
298 peak at 1113 cm^{-1} is ascribed to the stretching vibration of ether group (C-O-C). These
299 characteristic peaks all increased with the increase of PU prepolymer concentration.

300 **Figure 11(a)** and **Figure 11(b)** show the infrared spectra of mineral filler and PU
301 asphalt mastic. The peak at 3500 cm^{-1} in **Figure 11(a)** corresponds to hydroxyl groups (-
302 OH). The mineral filler had been heated in oven at $150\text{ }^{\circ}\text{C}$ for 4 hours to remove moisture.
303 Thus, the hydroxyl groups should come from the mineral filler. In fact, it was reported
304 that the surface atoms of mineral aggregate are attached with hydroxyl groups (-OH) (Gao
305 et al., 2019, Zaidi et al., 2020). The hydroxyl groups can react with the isocyanate group
306 (-NCO) in PU prepolymer. To confirm the hypothesis, PUMB-10 was mixed with the
307 dried mineral filler to prepare the PU asphalt mastic and kept in an oven at $60\text{ }^{\circ}\text{C}$ for up
308 to 48 h. The infrared spectra of the mastic during the conditioning were evaluated at 0 h,
309 12 h, 24 h, and 48 h, as demonstrated in **Figure 11(b)**. It can be seen that the distinct peak
310 at 2270 cm^{-1} ascribed to the isocyanate group of PU prepolymer decreased continuously
311 in this process, while the peak at around 3300 cm^{-1} corresponding to amino group
312 increased. The NCO peak intensity dropped significantly during the first 12 h, and then
313 decreased slowly. The results indicated that the chemical reaction between PU
314 prepolymer with the surface hydroxyl groups proceeded rapidly during the first 12 h,
315 which then slowed down due to the decreasing concentration of PU prepolymer and the
316 hydroxyl group on mineral filler. It is thus inferred that the PU prepolymer reacts majorly
317 with the surface hydroxyl group on aggregate surface.

318 **Figure 12** shows the schematic representation of the chemical reaction between
319 PU prepolymer and aggregate. The isocyanate group of the PU prepolymer reacts with
320 the surface hydroxyl group of aggregate, which forms the urethane group (-NHCOO-).
321 Thus, the peak for isocyanate group decreased while the peak for amino group increased
322 during this process as shown in **Figure 11(b)**. With the curing reaction between the PU
323 prepolymer and the surface hydroxyl group of aggregate, the three-dimensional PU
324 polymer network will be formed in the asphalt mixture as shown in **Figure 13**, which

325 leads to the improvement of the overall mechanical performance of the PU modified
326 asphalt mixture.

327 **6 Conclusions and recommendations**

328 This study investigated the performance of asphalt mixture modified by one-component
329 PU (PU prepolymer), and explored the PU modification mechanism, through various
330 laboratory tests. The following points summarize the main conclusions of this study:

- 331 • PU prepolymer can decrease the viscosity of base bitumen, and the chemical
332 reaction between PU prepolymer and bitumen is negligible.
- 333 • The overall performances of asphalt mixture were increased significantly by
334 PU prepolymer, including increased Marshall stability, ITS, and resistance to
335 moisture damage, rutting and fatigue damage.
- 336 • PU prepolymer can react with the hydroxyl groups on aggregate surface,
337 which contributes to the improved performances of asphalt mixture.

338 For the future studies, life cycle cost analysis (LCCA) will be performed and the
339 environmental impacts of PUMA will be systematically investigated to justify the
340 applications of PUMA in different scenarios.

341 **Declarations of interest: none.**

342 **References**

- 343 AIREY, G. 2003. Rheological properties of styrene butadiene styrene polymer modified
344 road bitumens. *Fuel*, 82, 1709-1719.
- 345 APOSTOLIDIS, P., LIU, X., KASBERGEN, C., VAN DE VEN, M. F. C.,
346 PIPINTAKOS, G. & SCARPAS, A. 2018. Chemo-Rheological Study of
347 Hardening of Epoxy Modified Bituminous Binders with the Finite Element
348 Method. *Transportation Research Record*, 2672, 190-199.
- 349 CAO, R., LENG, Z., YU, H. & HSU, S.-C. 2019. Comparative life cycle assessment of
350 warm mix technologies in asphalt rubber pavements with uncertainty analysis.
351 *Resources, Conservation and Recycling*, 147, 137-144.
- 352 CHEN, J., YIN, X., WANG, H. & DING, Y. 2018. Evaluation of durability and
353 functional performance of porous polyurethane mixture in porous pavement.
354 *Journal of Cleaner Production*, 188, 12-19.

- 355 CONG, L., YANG, F., GUO, G., REN, M., SHI, J. & TAN, L. 2019. The use of
356 polyurethane for asphalt pavement engineering applications: A state-of-the-art
357 review. *Construction and Building Materials*, 225, 1012-1025.
- 358 FANG, C., YU, X., YU, R., LIU, P. & QIAO, X. 2016. Preparation and properties of
359 isocyanate and nano particles composite modified asphalt. *Construction and
360 Building Materials*, 119, 113-118.
- 361 GAO, Y., ZHANG, Y., YANG, Y., ZHANG, J. & GU, F. 2019. Molecular dynamics
362 investigation of interfacial adhesion between oxidised bitumen and mineral
363 surfaces. *Applied Surface Science*, 479, 449-462.
- 364 HONG, B., LU, G., GAO, J., DONG, S. & WANG, D. 2021a. Green tunnel pavement:
365 Polyurethane ultra-thin friction course and its performance characterization.
366 *Journal of Cleaner Production*, 289.
- 367 HONG, B., LU, G., GAO, J. & WANG, D. 2021b. Evaluation of polyurethane dense
368 graded concrete prepared using the vacuum assisted resin transfer molding
369 technology. *Construction and Building Materials*, 269.
- 370 JIN, X., GUO, N., YOU, Z., WANG, L., WEN, Y. & TAN, Y. 2020. Rheological
371 properties and micro-characteristics of polyurethane composite modified
372 asphalt. *Construction and Building Materials*, 234.
- 373 LENG, Z., PADHAN, R. K. & SREERAM, A. 2018. Production of a sustainable paving
374 material through chemical recycling of waste PET into crumb rubber modified
375 asphalt. *Journal of Cleaner Production*, 180, 682-688.
- 376 LI, T., CARREÑO GÓMEZ, N. H., LU, G., LIANG, D., WANG, D. & OESER, M.
377 2021. Use of Polyurethane Precursor-Based Modifier as an Eco-Friendly
378 Approach to Improve Performance of Asphalt. *Journal of Transportation
379 Engineering, Part B: Pavements*, 147.
- 380 LI, T., GUO, Z., LIANG, D., LUO, S., ZHANG, Y., HONG, B., LU, G., WANG, D. &
381 OESER, M. 2022. Chemical and physical effects of polyurethane-precursor-
382 based reactive modifier on the low-temperature performance of bitumen.
383 *Construction and Building Materials*, 328.
- 384 LU, G., RENKEN, L., LI, T., WANG, D., LI, H. & OESER, M. 2019. Experimental
385 study on the polyurethane-bound pervious mixtures in the application of
386 permeable pavements. *Construction and Building Materials*, 202, 838-850.
- 387 SI, J., JIA, Z., WANG, J., YU, X., LI, Y., DONG, F. & JIANG, R. 2018. Comparative
388 analysis of cold-mixed epoxy and epoxy SBS-modified asphalts: Curing
389 rheology, thermal, and mechanical properties. *Construction and Building
390 Materials*, 176, 165-171.
- 391 SINGH, B., TARANNUM, H. & GUPTA, M. 2003. Use of isocyanate production
392 waste in the preparation of improved waterproofing bitumen. *Journal of Applied
393 Polymer Science*, 90, 1365-1377.
- 394 WANG, H., LIU, X., APOSTOLIDIS, P. & SCARPAS, T. 2018. Review of warm mix
395 rubberized asphalt concrete: Towards a sustainable paving technology. *Journal
396 of Cleaner Production*, 177, 302-314.
- 397 WANG, H., LIU, X., APOSTOLIDIS, P., WANG, D., LENG, Z., LU, G., ERKENS, S.
398 & SKARPAS, A. 2021. Investigating the High- and Low-Temperature
399 Performance of Warm Crumb Rubber-Modified Bituminous Binders Using
400 Rheological Tests. *Journal of Transportation Engineering, Part B: Pavements*,
401 147.
- 402 WANG, H., LIU, X., ERKENS, S. & SKARPAS, A. 2020a. Experimental
403 characterization of storage stability of crumb rubber modified bitumen with
404 warm-mix additives. *Construction and Building Materials*, 249.

405 WANG, H., LIU, X., VAN DE VEN, M., LU, G., ERKENS, S. & SKARPAS, A.
406 2020b. Fatigue performance of long-term aged crumb rubber modified bitumen
407 containing warm-mix additives. *Construction and Building Materials*, 239.
408 YANG, F., CONG, L., LI, Z., YUAN, J., GUO, G. & TAN, L. 2022. Study on
409 preparation and performance of a thermosetting polyurethane modified asphalt
410 binder for bridge deck pavements. *Construction and Building Materials*, 326.
411 ZAIDI, S. B. A., AIREY, G. D., GRENFELL, J., AHMAD, N. & AHMED, I. 2020.
412 Moisture susceptibility assessment of hydrated lime modified asphalt mixture
413 and surface energy. *International Journal of Pavement Engineering*, 1-13.
414 ZHU, J., BALIEU, R. & WANG, H. 2019. The use of solubility parameters and free
415 energy theory for phase behaviour of polymer-modified bitumen: a review. *Road*
416 *Materials and Pavement Design*, 22, 757-778.

417

418

419

420

421

422

423

424

425

426

427

428

429

430

431

432

433

434

435

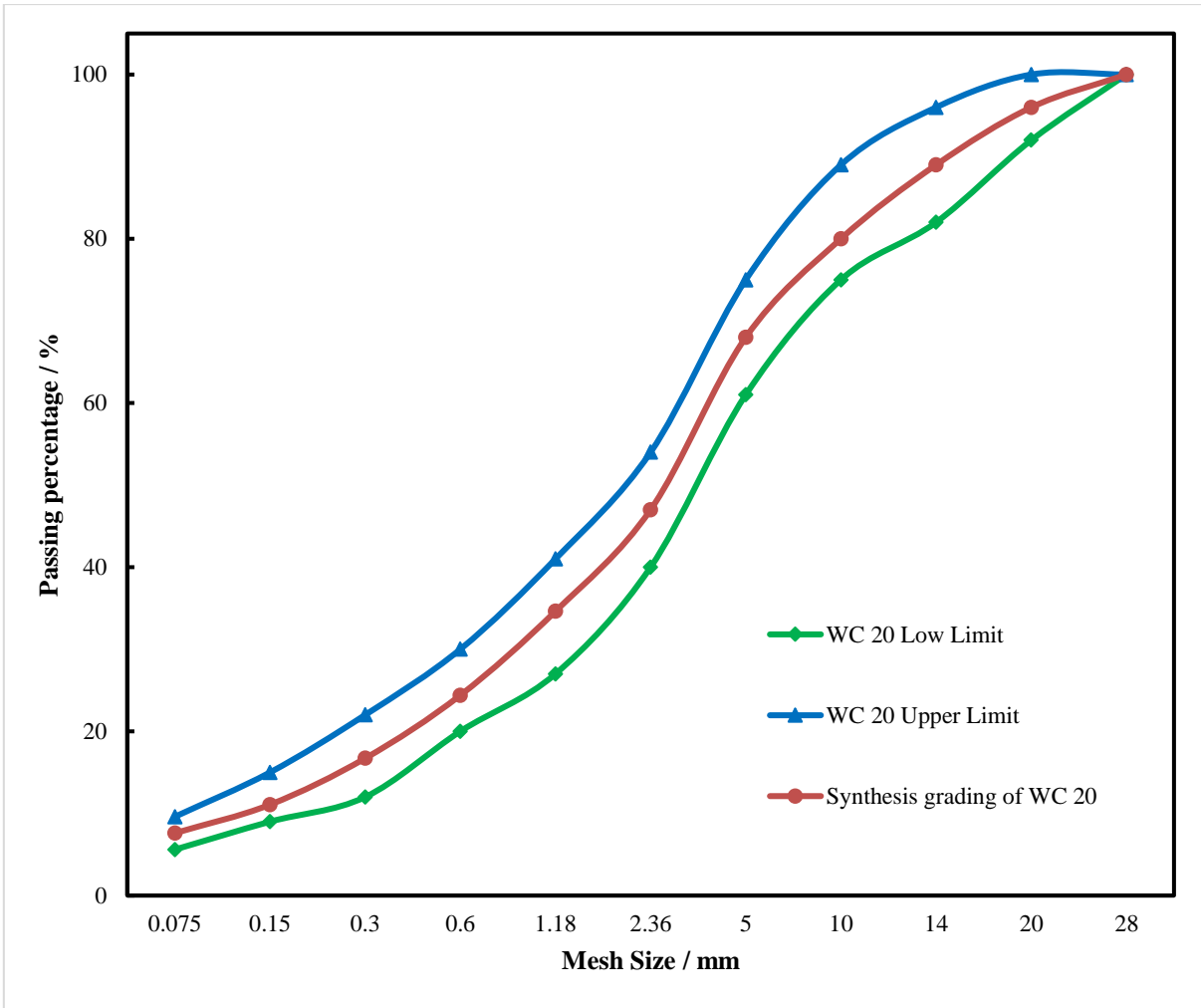


Fig. 1 Grain size distribution of WC 20

436
437
438

439

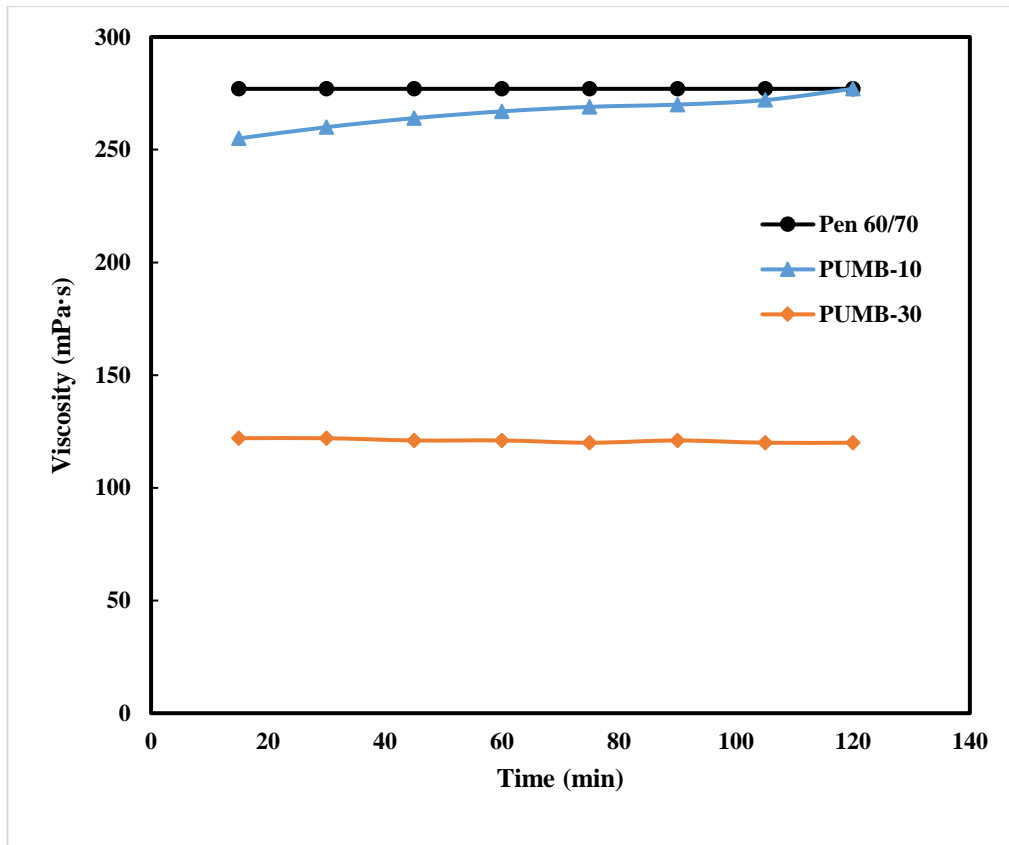


Fig. 2 Rotational viscosity of PU modified bitumen with time

440

441

442

443

444

445

446

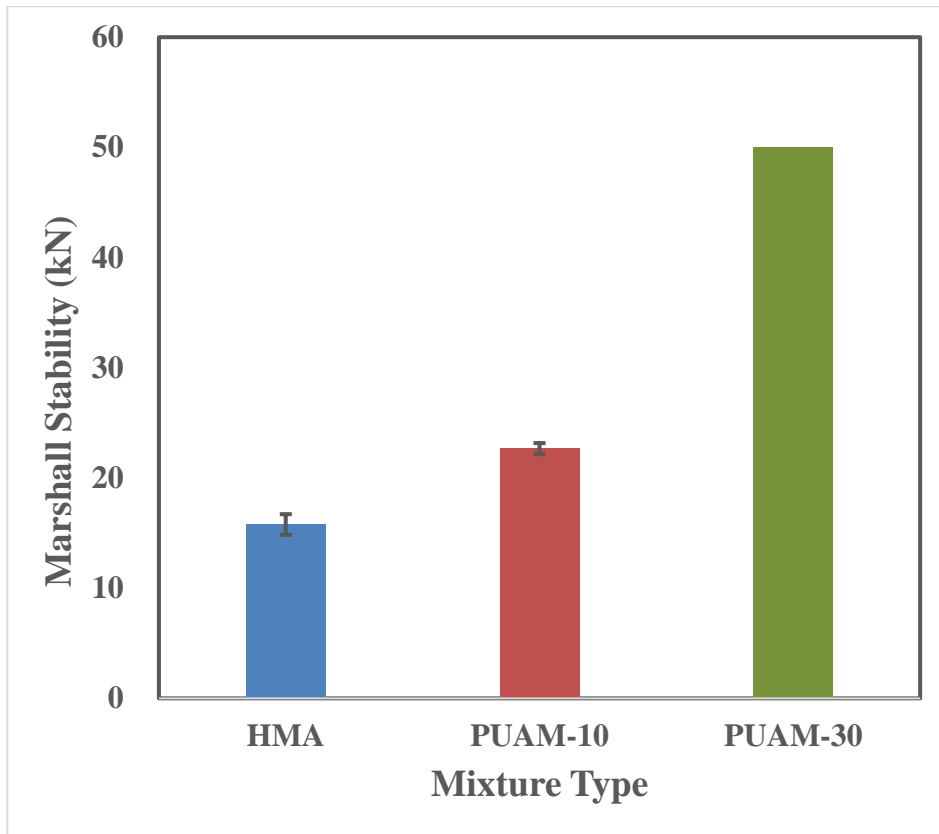


Fig. 3. Marshall tests results of PUMA and HMA

447
448
449

450

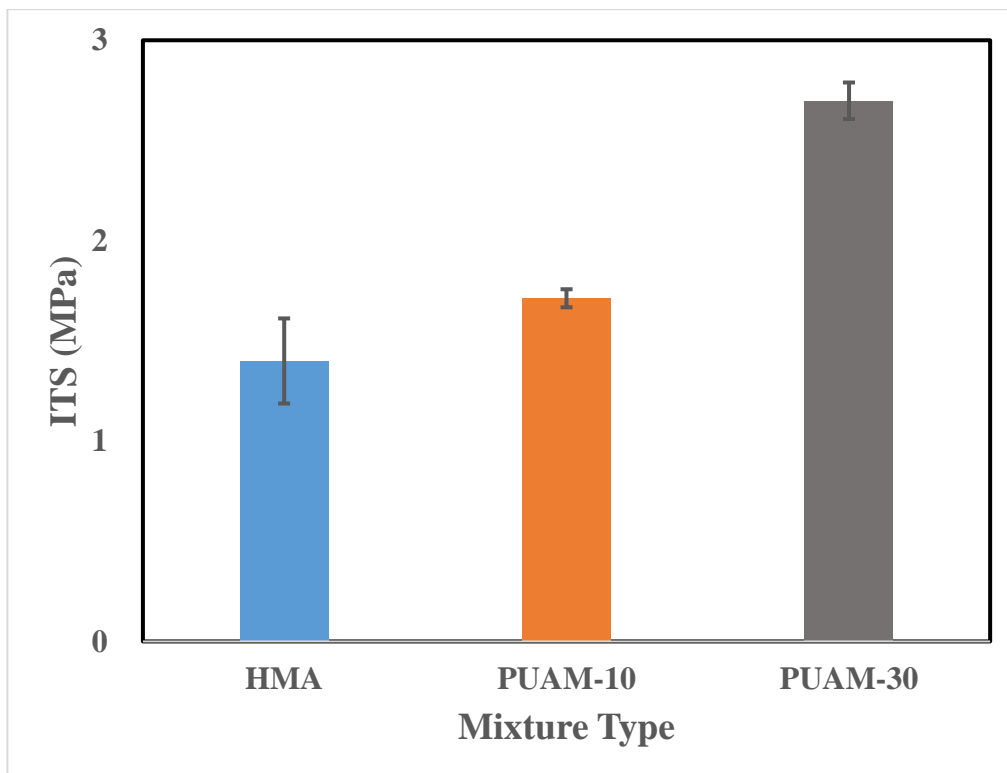


Fig. 4. ITS results of PUAM and HMA

451
452
453

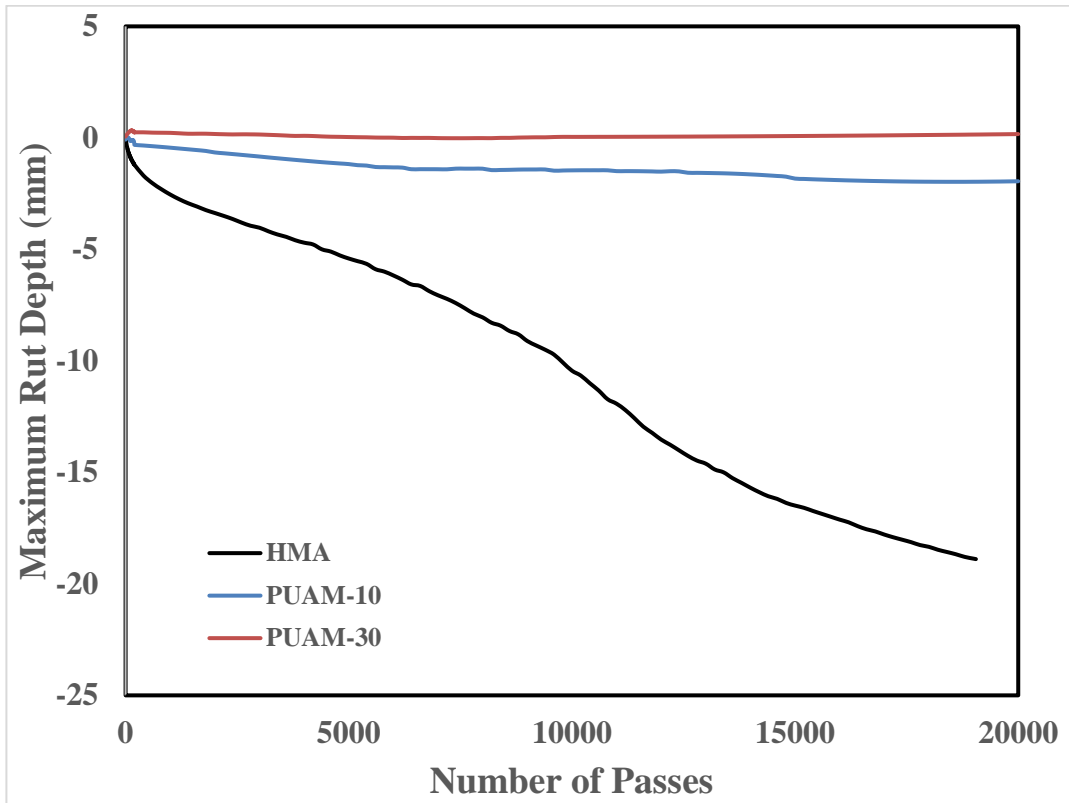


Fig. 5. Rut depths of different asphalt mixtures during wheel-tracking tests

455
456
457
458
459
460
461
462

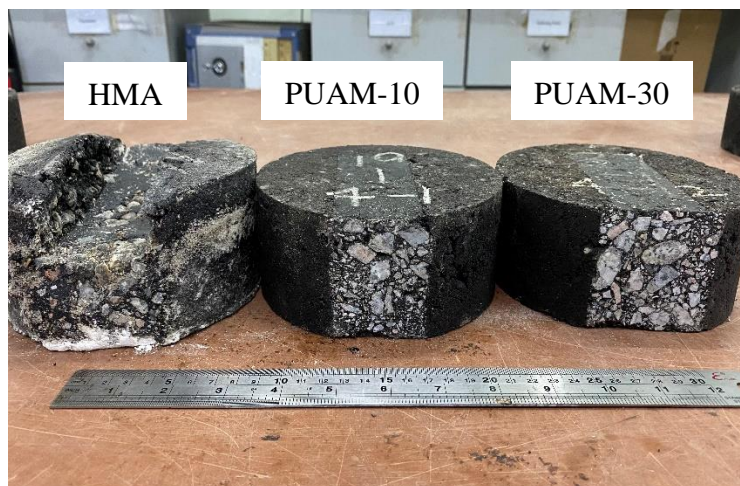


Fig. 6. Test samples after the wheel-tracking test

463
464
465
466
467
468

469
470
471
472

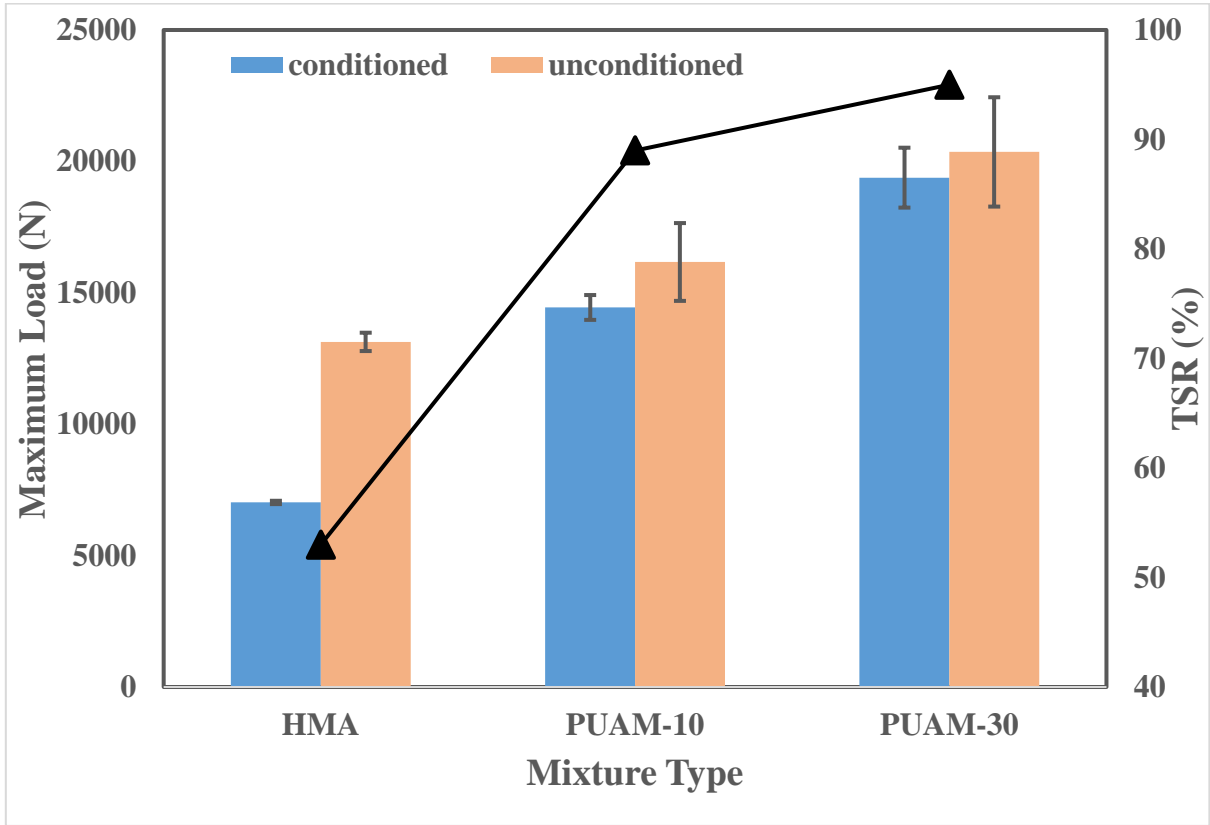


Fig. 7. Moisture susceptibility results

473
474
475
476
477

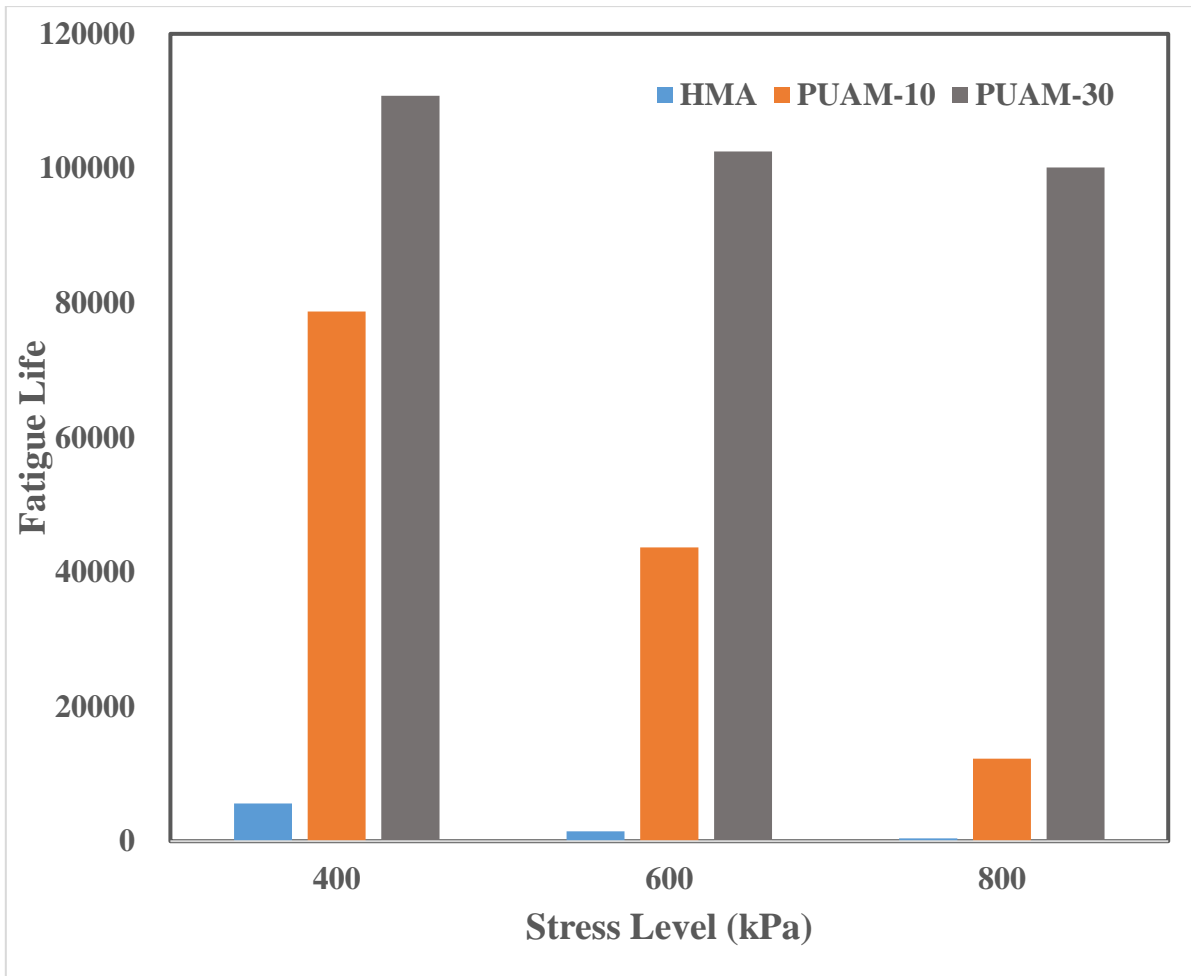
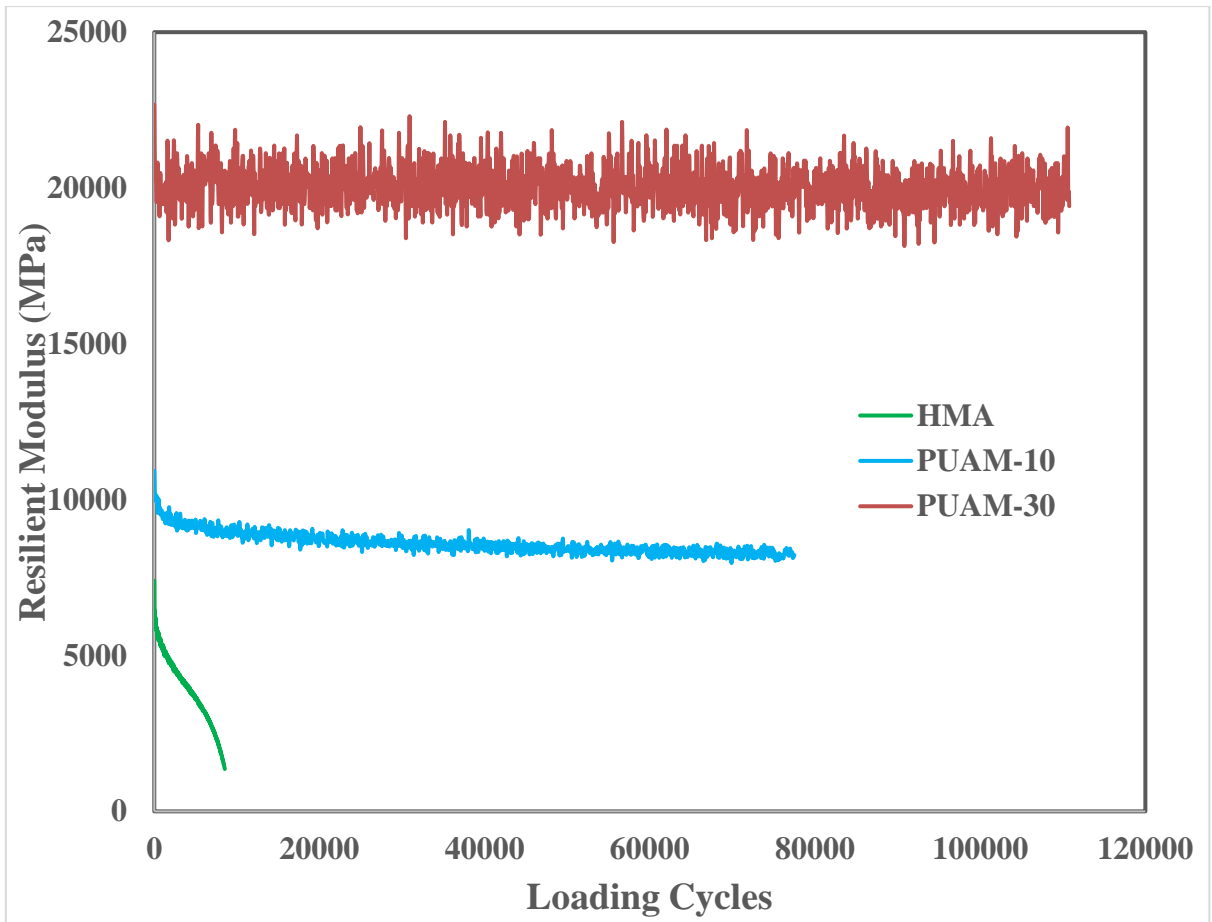


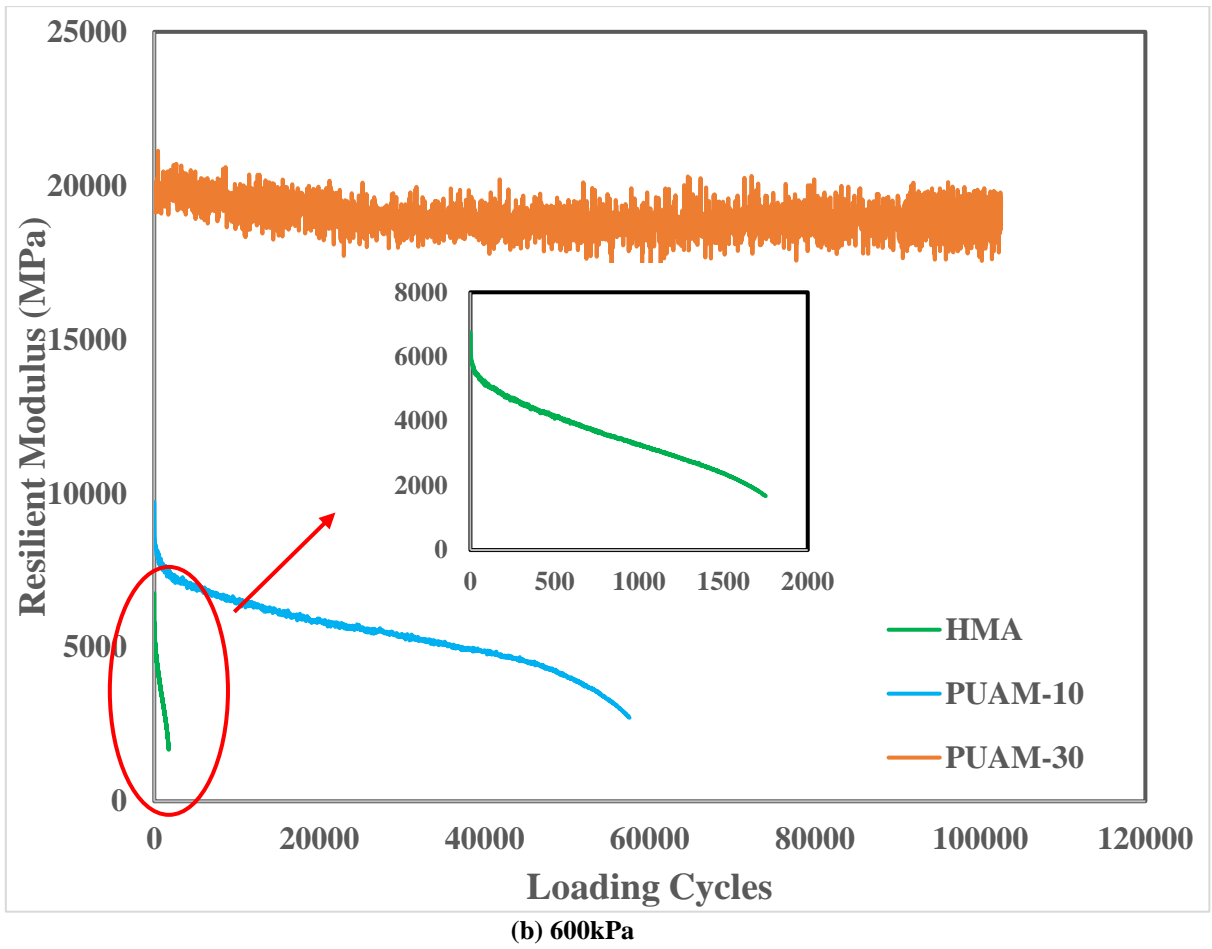
Fig. 8. Fatigue lives of PUMA and HMA under different stress levels

478
 479
 480
 481
 482
 483
 484

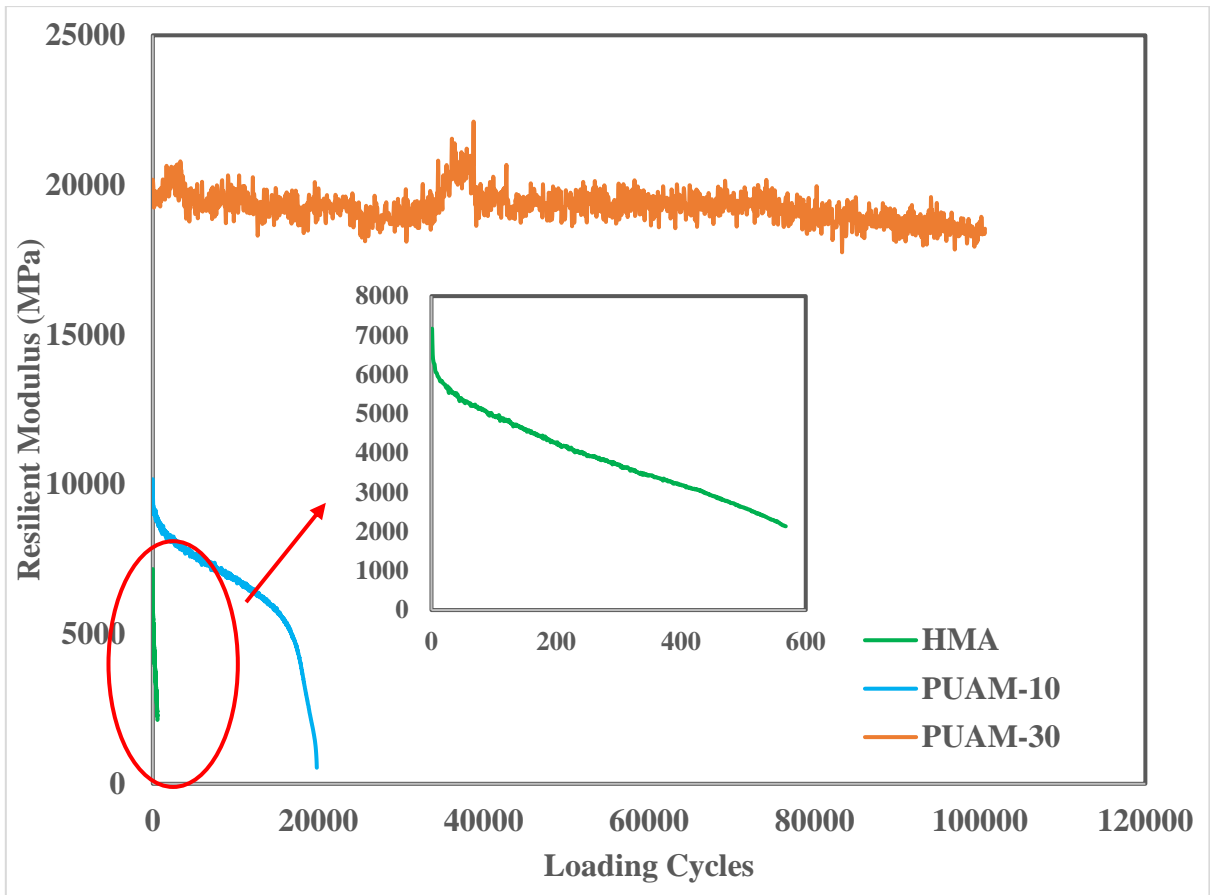


(a) 400kPa

485
486



487
488
489



(c) 800kPa

Fig. 9. Resilient modulus vs. loading cycles under each stress level (a) 400kPa (b) 600kPa (c) 800kPa

490
491
492
493
494
495
496
497
498
499
500

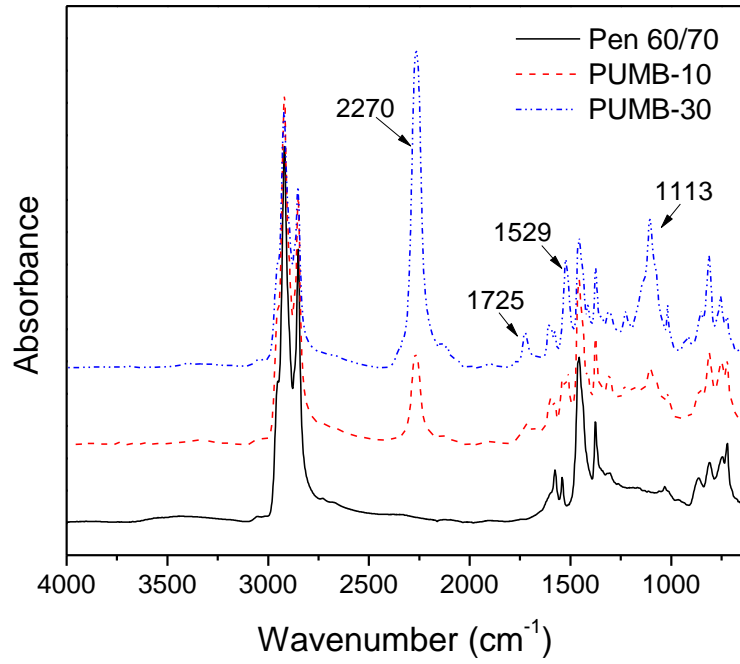


Fig. 10 FT-IR spectra of Pen 60/70 and PU modified bitumen binders

501
502
503
504
505

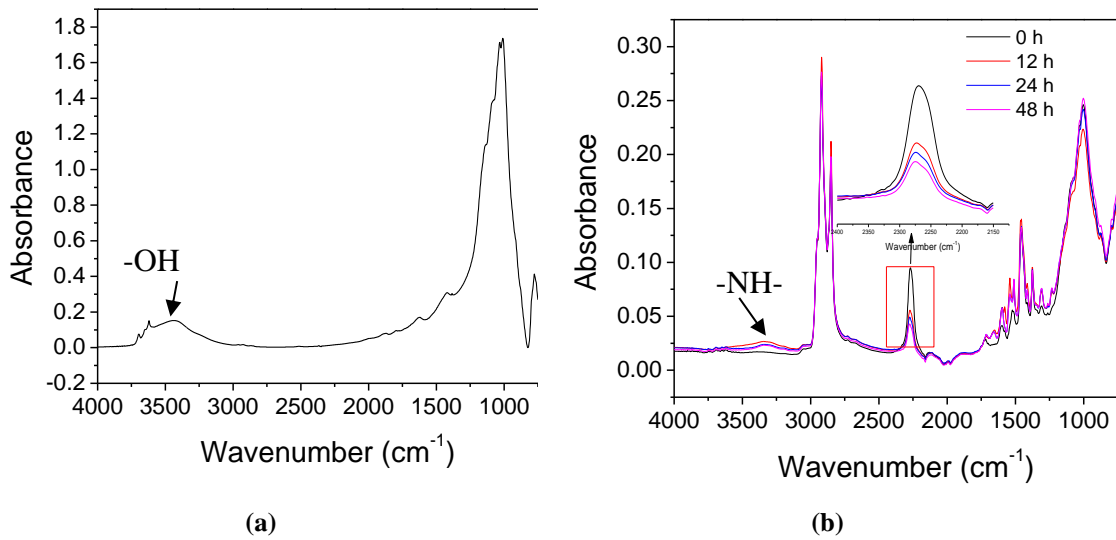
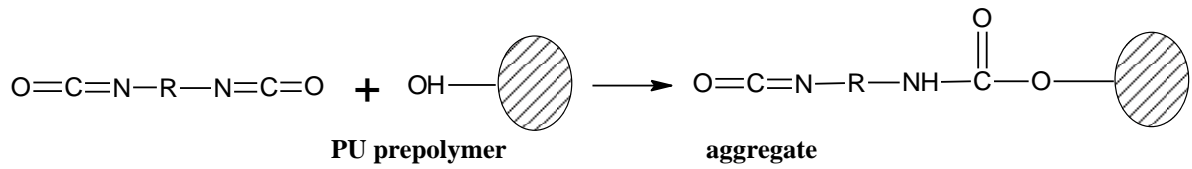


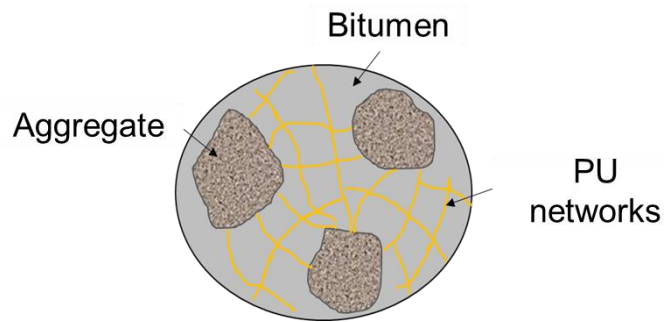
Fig. 11 Infrared spectra of (a) mineral filler, and (b) PU asphalt mastic

506
507
508
509
510



511
512
513
514
515
516
517
518
519
520
521
522
523

Fig. 12 Schematic representation of the chemical reaction between PU prepolymer and mineral aggregate



524
525
526
527

Fig. 13 Schematic illustration of the PU polymer network formed between bitumen and aggregate.

528
529
530
531
532
533
534
535
536
537
538
539

540
541
542
543
544
545
546
547
548
549
550
551
552
553
554
555
556
557
558
559
560
561
562
563
564
565
566

Table 1 Properties of PU prepolymer

Characteristics	Unit	Value	Method
Density (25°C)	kg/m ³	1120	G 133-08
Viscosity	mPa·s	4200	G 133-07
NCO content	%	15.5	G 133-06
Shelf-life	month	6	-

Table 2 Basic properties of Pen 60/70 binder

Properties	Value	Specification
Penetration (25°C, 0.1mm)	64.5	ASTM D5
Softening Point (°C)	48.5	ASTM D36
Viscosity at 135°C (mPa·s)	477.5	ASTM 4402
Ductility at 25°C (cm)	78.5	ASTM D113
SARA fraction	Saturate	17.58 wt %
	Aromatic	46.85 wt %
	Resin	26.20 wt %
	Asphaltene	9.37 wt %
		ASTM 4124

Table 3 Rotational viscosity of binders at 150 °C

Sample-ID	Shear viscosity (mPa·s)
Pen 60/70	264
PUMB-10	260
PUMB-30	120

567
568
569
570

Table 4 Marshall and volumetric results of PUAM and HMA.

Test items	Mixture Type		
	HMA	PUAM-10	PUAM-30
Bulk density (g/cm ³)	2.33	2.31	2.30
Marshall Stability (KN)	15.8	22.7	>50
Flow Value (0.1mm)	2.12	1.83	NA
VA (%)	3.47	4.40	5.03
VMA (%)	16.4	17.0	17.7
VFA (%)	79.0	76.6	71.8

571
572
573
574

Table 5 Band assignment PU modified bitumen binders

Wavenumber (cm ⁻¹)	Band assignment
1113	C-O-C stretching
1529	N-H bending (amide)
1725	C=O stretching (amide)
2270	N=C=O stretching
2873	C-H stretching (CH ₂)
2927	C-H stretching (CH ₃)

575

576

577